



Comparison of dose distributions in target areas and organs at risk in conformal and VMAT techniques and dose verifications with the use of thermoluminescence dosimetry

Monika Paluch-Ferszt ,
Beata Kozłowska,
Marcin Dybek

Abstract. The aim of the present study is to compare dose distributions and their verification in target areas and organs at risk (OAR) in conformal and volumetric modulated arc therapy (VMAT) techniques. Proper verification procedures allow the removal of the major sources of errors, such as incorrect application of a planning system, its insufficient or cursory commissioning, as well as an erroneous interpretation of the obtained results. Three target areas (head and neck, chest, and pelvic) were selected and the treatment was delivered based on plans made using collapsed cone convolution and Monte Carlo algorithms with 6-MV photon beams, adopting conformal and VMAT techniques, respectively. All the plans were prepared for the anthropomorphic phantom. Dose measurements were performed with TL detectors made of LiF phosphor doped with magnesium and titanium (LiF:Mg,Ti). This paper presents the results of TL measurements and calculated doses, as well as their deviations from the treatment planning system (TPS) in the three planned target areas. It was established that the algorithms subject to analysis differ, particularly in dose calculations for highly inhomogeneous regions (OAR). Aside from the need to achieve the dose intended for the tumour, the choice of irradiation technique in teletherapy should be dictated by the degree of exposure to individual critical organs during irradiation. While nothing deviated beyond the bounds of what is acceptable by international regulatory bodies in plans from TPS, clinically one must be more cautious with the OAR areas.

Keywords: Collapsed cone convolution algorithm • Monte Carlo algorithm • Organ at risk (OAR) • Thermoluminescent dosimeter (TLD) • Treatment planning system

M. Paluch-Ferszt 
Heavy Ion Laboratory
University of Warsaw
Pasteura 5A, 02-093 Warszawa, Poland
and Institute of Physics
University of Silesia
75 Pulku Piechoty 1A, 41-500 Chorzow, Poland
E-mail: mpaluchferszt@gmail.com

B. Kozłowska
Institute of Physics
University of Silesia
75 Pulku Piechoty 1A, 41-500 Chorzow, Poland

M. Dybek
Radiotherapy Department
Katowice Oncology Center
Raciborska 27, 40-074 Katowice, Poland

Received: 19 November 2019
Accepted: 27 August 2020

Introduction

The radiation doses calculated using the treatment planning systems (TPSs) depend on the type of applied dose calculation algorithms. At present, Monte Carlo (MC) simulation is the most sophisticated and accurate algorithm and it is used as the generation of benchmark dose distribution. These doses serve as the basis for comparison of the results of other less accurate computerized dose calculation methods [1–3]. Proper verification procedures allow removal of the major sources of errors, such as incorrect application of a planning system, its insufficient or cursory commissioning, as well as an erroneous interpretation of the obtained results [4].

Numerous problems in radiation dosimetry, radiotherapy physics and radiation protection have been addressed through the use of MC techniques, because the complexity of electron and photon transport in material makes analytical solutions difficult to solve. The MC method uses photon and electron transport physics to consider the trajectories of individual particles, and thus the pattern of dose deposition. Each particle's history is determined by the random number generator and millions of particles' histories are traced. The dose distribution is built by summing

up the energy deposition in each particle's history [5]. Although MC techniques are quite useful in dose calculations, they are very intensive computationally and therefore, other calculation algorithms are also used.

Another algorithm used for dose calculations in TPS is the collapsed cone convolution (CCC). This dose calculation algorithm is based on a separation of the primary photon transport and secondary transport of photons and electrons. The total energy released per unit mass (TERMA) represents the primary photon transport. TERMA is the total energy released in material. Point-spread kernels $h(E, s, r)$ represent the secondary transport of electrons and photons. They give rise to the distribution of energy or dose to a point r from a single photon interaction at a point s in water. The point-spread kernels are often pre-calculated with MC simulations for discrete energies. The CCC dose algorithm decreases the computational time by collapsing the kernels into a certain number of directions. The total energy E or dose is allocated to rectilinear directions emerging from the interaction point. This efficiently simplifies and reduces the number of scatter directions from the kernel h [6].

However, some reports show large deviations for the absolute dose (dose/monitor unit) which occur in regions of electronic disequilibrium for the CCC algorithm used [7].

Dose calculation depends on the algorithm used in TPS. In the Radiotherapy Department of the Katowice Oncology Center, dose calculations for patients treated with external photon beams have been routinely performed using the Oncentra MasterPlan (Version 4.3) TPS for conformal and Monaco (Version 3.30.01) TPS for VMAT techniques. They calculate doses on the basis of CCC and MC algorithms, respectively.

The aim of this publication is to compare these two algorithms and verify the results by measuring the doses in target areas (head and neck, chest, and pelvic) and their respective organs at risk (OAR). Errors in these algorithms can lead to increased doses to OAR as well as not enough radiation to the tumour.

The doses absorbed in the targets and selected organs were evaluated using the anthropomorphic phantom ATOM® (CIRS – Computer Imaging Reference Systems, Inc.) and thermoluminescent detectors (TLD).

Materials and methods

The measurements were performed with LiF:Mg,Ti TL detectors (MTS-N, TLD Poland) in the form of cylindrical pellets with a diameter of 4.5 mm, a thickness of 0.8 mm and the effective atomic number $Z_{\text{eff}} = 8.14$. The TL response of pellets was acquired by the RA'04 TLD reader system manufactured in Poland. Prior to each main read-out, the pellets were annealed in a furnace in two phases: first at the temperature of 400°C for 1 h and then at 100°C for 2 h. Next, they were cooled rapidly by transferring them on top of an aluminium block at room temperature. The scheme for pellets treatment was

as follows: annealing – TL read-out for background reduction – irradiation – TL read-out – annealing.

Prior to the phantom dose measurements, each detector underwent calibration in reference conditions using beams of the same radiation quality as used in treatment planning. The calibration during emission of therapeutic photon beam was performed on an accelerator with a nominal energy of 6 MV, skin surface distance (SSD) of 100 cm and field size of $10 \times 10 \text{ cm}^2$. For the purposes of calibration, special holes to contain TLD pellets were made in a solid water slab (density of 1.02 g/cm^3). The holes were arranged symmetrically around the slab centre within a 10-cm square field. A cylindrical Farmer-type ionization chamber of 0.6 cm^3 volume was used as a reference dosimeter for TLDs calibration; it was also used for comparison of the read-outs. All calibrated detectors had to be exposed to the calibration dose at the same time to minimize differences in irradiation conditions, and thus differences in future dose read-outs.

The patient (adult male) was simulated by the ATOM® phantom from CIRS. Its image was obtained using Siemens CT-Scan and then was copied to the radiotherapy planning system for the purposes of the conformal and VMAT optimization techniques.

Given the objectives of this study, three treatment plans were prepared for three selected target areas: (a) head and neck, (b) chest, and (c) pelvic for conformal and VMAT techniques. The planned treatment was delivered with 6-MV beams for both radiotherapy techniques. A dose comparison for individual points for the two different treatment techniques could be made because the plans concerned the same localization of the isocentres. The doses were calculated using the CCC and MC algorithms. The doses calculated for the anthropomorphic phantom with the use of two algorithms were compared with the doses measured with calibrated TLD pellets placed inside the phantom during the irradiation.

Head and neck area

In the head and neck area, a hypothetical clinical target volume (CTV) equal to 31.62 cm^3 with a planning target volume (PTV) of 11.447 cm^3 was located in the brain. The OARs in this case were the brain, brainstem, right eye and left eye. A treatment plan was created with five noncoplanar beams in the conformal technique and 144 plan segments in the VMAT technique. The total planned dose for the target volume was about 54 Gy and it was given in 27 fractionations (2 Gy). The final plan required 186 MUs per gray of prescribed dose in the conformal technique and 394 MUs per gray in the VMAT technique.

Chest area

In the chest area, the CTV was equal to 51.3 cm^3 , the PTV was 180.3 cm^3 and it was located in the left lung. The OARs in this case were as follows: the right lung, heart, spinal canal, vertebral arch and vertebral body.

A treatment plan was created with four noncoplanar beams/56 plan segments. The total planned dose for the target volume was about 46 Gy and it was given in 23 fractionations (2 Gy). The final plan required 286 MUs in the conformal technique and 320 MUs per gray of prescribed dose in the VMAT technique.

Pelvic area

In the pelvic area, the CTV was equal to 49.78 cm³, the PTV equaled 155.55 cm³ and it was located in the prostate. The OARs in this case were the bladder, rectum, right femoral head and left femoral head. A treatment plan was developed with five noncoplanar beams/54 plan segments with the prescribed dose of 76 Gy (2 Gy/fraction, 38 fractions). The final plan required 174 MUs in the conformal and 304 MUs per gray of prescribed dose in the VMAT technique.

The TLDs were placed at different points within the irradiated area, in sets of three per each point with a view to checking the repeatability of the measurements. The location of the points was selected so as to include three different dose distribution regions: target area, CTV, PTV and OAR. Figures 1–3 illustrate in detail the locations of the measurement points for three regions: head and neck, chest, and pelvic. The dose measured at a single point within a structure was an arithmetic mean of the read-outs of the three detectors placed at that point.

In order to evaluate and analyse the data, the formula as indicated in AAPM Task Group 119 was used. The dose difference (*D* in %) was calculated as

$$(1) \quad D = \frac{D_{PLAN} - D_{TLD}}{D_{PLAN}} \cdot 100\%$$

where *D*_{PLAN} is the planned dose at TPS and *D*_{TLD} is the mean measured dose in the detectors. Later, the results of the calculations were evaluated in accordance with the International Atomic Energy Agency (IAEA) recommendations and criteria [1].

Results and discussion

The analyses of the results for the cases presented in Figs. 1–3 were carried out based on the international

recommendations of IAEA [1] and the European Society for Radiotherapy and Oncology (ESTRO) [8]. The maximum accepted deviations of dose values, as calculated by the computerized TPS from the actual doses measured in selected regions of a certain photon field, were determined as stipulated in the above recommendations. Tables 1–3 present the results obtained in the selected target areas.

Head and neck area

When analysing the data in the conformal technique at the points of the CTV area presented in Table 1, it must be observed that the differences (*D*) between the TPS-calculated doses and TLD-measured doses were in a range from –1.45% (3wk) to a maximum of –2.45% (2wk). This means that the doses measured by the detectors were higher than the doses calculated by the treatment plan. In clinical practice, as defined in various international recommendations such as IAEA [1] and ESTRO [8], the difference between the scheduled dose and the dose obtained by a patient should not exceed 5%. TL detectors absorbed doses similar to those planned by the treatment plan.

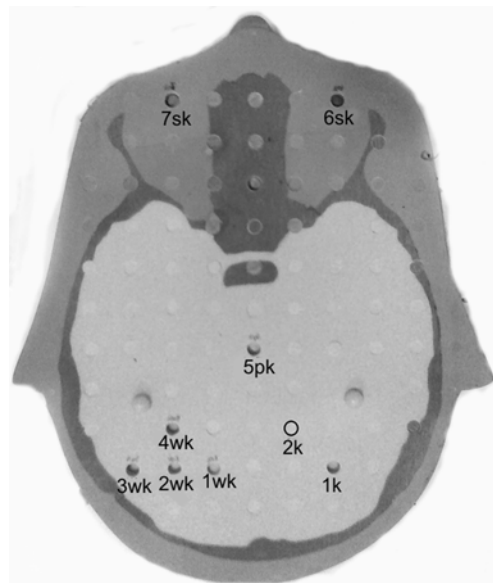


Fig. 1. Location of the measurement points from the phantom head and neck area described in Table 1.

Table 1. Results of the measurements and deviations of the TPS calculated doses from the measured ones for the planned target head and neck area

Location	No.	<i>D</i> _{PLANc} [Gy]	<i>D</i> _{TLD} [Gy] ± σ <i>D</i> _{TLD} [%]	Δ _c [%]	<i>D</i> _{PLANv} [Gy] ± σ <i>D</i> _{PLANv} [%]	<i>D</i> _{TLD} [Gy] ± σ <i>D</i> _{TLD} [%]	Δ _v [%]
Brain	1k	1.51	1.49 (2.87)	1.32	1.12 (2.03)	1.16 (2.79)	–3.57
Brain	2k	1.14	1.12 (2.38)	1.75	1.15 (2.26)	1.18 (2.25)	–2.61
CTV	1wk	2.07	2.12 (2.28)	–2.42	2.08 (0.86)	2.11 (1.82)	–1.44
CTV	2wk	2.04	2.09 (2.88)	–2.45	2.07 (0.98)	2.13 (1.98)	–2.90
CTV	3wk	2.07	2.10 (2.02)	–1.45	2.08 (1.06)	2.15 (1.28)	–3.37
CTV	4wk	2.07	2.11 (1.17)	–1.93	2.09 (0.67)	2.15 (1.10)	–2.87
Brainstem	5pk	0.54	0.56 (3.55)	–3.70	0.89 (4.36)	0.91 (2.30)	–2.25
Left eye	6sk	0.02	0.021 (2.11)	–5.00	0.018 (5.26)	0.019 (2.38)	–5.56
Right eye	7sk	0.06	0.059 (1.96)	1.67	0.049 (2.96)	0.047 (2.87)	4.08

*D*_{PLANc} – dose calculated using CCC algorithm, *D*_{PLANv} – dose calculated using Monte Carlo algorithm, *D*_{TLD} – dose measured with TLDs, Δ_{c,v} – percentage deviation of TLD measured dose from the calculated by the planning system.

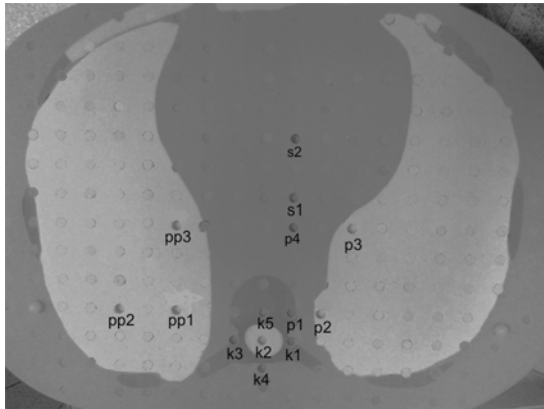


Fig. 2. Location of the measurement points from the phantom chest area described in Table 2.

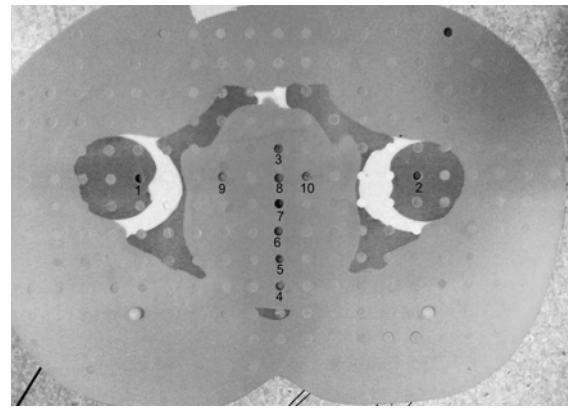


Fig. 3. Location of the measurement points from the phantom pelvic area described in Table 3.

The biggest difference in critical organs was observed in the left eye, where the difference between doses was -5.00% (6sk). The smallest difference in the doses emerged in the brain (1k) and was equal to 1.32% . It should be noted that the obtained results did not take into account the measurement uncertainties (σ) of the doses measured by TL detectors. The highest uncertainty (5pk) was 3.55% and the lowest (4wk) was 1.17% .

As regards the analysis of the VMAT data (Table 1) in the CTV area, the doses measured by the detectors were higher than the doses calculated by the treatment

plan by -1.44% (1wk) to a maximum value of -3.37% (3wk). These results met the clinical assumptions.

The biggest differences in critical organs can be seen in the left and right eyes (6sk and 7sk points), where the differences between doses were -5.56% and 4.08% , respectively. The smallest difference between the doses was in the brainstem (5pk), equal to -2.25% . In the case of VMAT, the measurement uncertainties of the TL detectors were lower than those in the conformal technique and ranged from a maximum value of 2.87% at 7sk to 1.10% at 4wk.

Table 2. Results of the measurements and deviations of the TPS calculated doses from the measured ones for the planned target chest area

Location	No.	D_{PLANc} [Gy]	D_{TLD} [Gy] $\pm \sigma D_{TLD}$ [%]	Δ_c [%]	D_{PLANv} [Gy] $\pm \sigma D_{PLANv}$ [%]	D_{TLD} [Gy] $\pm \sigma D_{TLD}$ [%]	Δ_v [%]
Heart	s1	1.91	1.96 (1.65)	-2.62	1.92 (0.63)	1.95 (1.73)	-1.56
Heart	s2	1.04	1.07 (3.92)	-2.88	0.79 (1.90)	0.81 (2.62)	-2.53
PTV	p1	1.88	1.95 (1.67)	-3.72	2.08 (2.16)	2.14 (1.54)	-2.88
CTV	p2	1.95	1.99 (1.66)	-2.05	2.09 (0.38)	2.18 (0.16)	-4.31
CTV	p3	1.98	2.09 (2.43)	-5.56	2.04 (0.39)	2.14 (0.30)	-4.90
PTV	p4	1.94	2.03 (1.70)	-4.64	2.01 (2.79)	2.08 (2.66)	-3.48
Right lung	pp1	0.69	0.71 (1.70)	-2.90	0.88 (3.31)	0.86 (4.09)	2.27
Right lung	pp2	0.57	0.58 (4.58)	-1.75	0.66 (5.34)	0.64 (4.95)	3.03
Right lung	pp3	0.51	0.52 (4.78)	-1.96	0.89 (3.49)	0.87 (3.52)	2.25
Vertebral arch	k1	1.70	1.74 (1.85)	-2.35	0.89 (2.13)	0.92 (2.57)	-3.37
Spinal canal	k2	1.10	1.12 (1.91)	-1.82	0.91 (1.86)	0.94 (1.89)	-3.30
Vertebral arch	k3	0.87	0.86 (4.19)	1.15	1.52 (0.79)	1.54 (2.16)	-1.32
Vertebral arch	k4	0.75	0.77 (4.51)	-2.67	0.83 (2.30)	0.84 (6.56)	-1.20
Vertebral arch	k5	1.30	1.32 (1.80)	-1.54	1.44 (0.62)	1.46 (1.16)	-1.39

Table 3. Results of the measurements and deviations of the TPS calculated doses from the measured ones for the planned target pelvic area

Location	No.	D_{PLANc} [Gy]	D_{TLD} [Gy] $\pm \sigma D_{TLD}$ [%]	Δ_c [%]	D_{PLANv} [Gy] $\pm \sigma D_{PLANv}$ [%]	D_{TLD} [Gy] $\pm \sigma D_{TLD}$ [%]	Δ_v [%]
Right femoral head	1	1.01	1.03 (2.83)	-1.98	0.93 (1.40)	0.96 (3.12)	-3.23
Left femoral head	2	0.97	0.98 (1.70)	-1.03	0.86 (1.51)	0.88 (2.69)	-2.33
CTV	3	2.02	2.10 (1.72)	-3.96	2.05 (0.29)	2.15 (1.45)	-4.88
Rectum	4	0.40	0.38 (1.01)	5.00	0.79 (1.65)	0.77 (2.08)	2.53
Rectum	5	1.40	1.36 (0.82)	2.86	1.01 (2.57)	0.99 (2.65)	1.98
Rectum	6	1.49	1.45 (1.66)	2.68	1.69 (4.49)	1.66 (1.63)	1.78
PTV	7	2.01	2.07 (0.80)	-2.99	2.05 (0.44)	2.12 (1.39)	-3.41
CTV	8	2.02	2.05 (0.57)	-1.49	2.06 (0.24)	2.12 (2.48)	-2.91
PTV	9	2.05	2.11 (0.17)	-2.93	2.06 (0.53)	2.11 (2.06)	-2.43
CTV	10	2.04	2.09 (2.85)	-2.45	2.03 (0.44)	2.11 (1.46)	-3.94

Chest area

In the chest area, the analysis of the data in the conformal technique (Table 2) reveals that the biggest differences (D) between the TPS-calculated doses and TLD-measured doses can be seen at the points of the CTV and PTV areas. The differences (D) were in a range from -2.05% (p2) to a maximum of -5.56% (p3). It has once again been found that the doses measured by the detectors were higher than the doses calculated by the treatment plan. The obtained values were on the borderline of the clinical assumptions.

The biggest difference in critical organs was observed in the heart (s1 and s2 points) where the values oscillate between -2.62% and -2.88% . The smallest difference in doses emerged in the vertebral arch (k3) and was equal to 1.15% . As in the head and neck case, the presented results did not take into account the measurement uncertainties (σ) of the doses measured by TL detectors. The highest uncertainty (pp3) was 4.78% and the lowest (s1) was 1.65% .

The analysis of the chest area data for VMAT (Table 2) shows that the biggest differences (D) can be seen at the points of the CTV and PTV areas. The doses measured by the detectors at these points were higher than the doses calculated by the treatment plan by -2.88% (p1), up to a maximum value of -4.9% (p3). These results met the clinical assumptions.

The biggest difference in critical organs can be seen in the vertebral arch (k4 and k1 points), where the differences between doses were -1.20% and 3.37% , respectively. The differences equal to -1.56% and -2.53% were present in the heart. The measurement uncertainties of the TL detectors were higher than those in the conformal technique and ranged from a maximum value of 6.56% at k4 to 0.16% at p2.

Pelvic area

In the pelvic area, the analysis of the data in the conformal technique (Table 3) reveals that the biggest differences (D) between the TPS-calculated doses and TLD-measured doses can be also seen at the points of the CTV and PTV areas. In this area (CTV: points 3, 8, 10, PTV: points 7, 9), the doses measured by the detectors were higher than the doses calculated by the treatment plan by -1.49% (point 8) up to -3.96% (point 3). The values met the clinical assumptions.

The biggest difference in critical organs was observed in the rectum (point 4), where the maximum value was equal to 5% . The smallest value equal to -1.03% was for the left femoral head (point 2). The presented results did not take into account the measurement uncertainties (σ) of doses measured by TL detectors. The highest uncertainty (point 10) was 2.85% and the lowest (point 9) was 0.17% .

The analysis of pelvic area data for VMAT (Table 3) shows that the biggest differences (D) can be once again seen at the points of the CTV and PTV areas. The doses measured by the detectors at

these points were higher than the doses calculated by the treatment plan by -2.43% (point 9) up to a maximum value of -4.88% (point 3). These results met the clinical assumptions.

The biggest difference in critical organs can be seen in the right femoral head (point 1) and it is equal to -3.23% , while the smallest difference was equal to 1.78% and was observed in the rectum (point 6). In the VMAT technique, the measurement uncertainties of the TL detectors were higher than those in the conformal technique and ranged from a maximum value of 3.12% at point 1 to 1.39% at point 7.

When comparing the treatment plans prepared for two treatment techniques, conformal and VMAT, differences in the dose rates in the target and in the OAR areas can be observed.

Head and neck area

When comparing the two treatment techniques we find that VMAT delivers a higher dose of 0.02 Gy in the target area and a dose of 0.36 Gy in an organ at risk such as the brainstem. However, if we take into account the criterion of eye and brain protection, the doses at these points were lower by 0.007 Gy and 0.19 Gy for VMAT.

It should be emphasized that the presented doses apply only to one irradiation fraction, and if all the fractions from the treatment plan are included (27 fractions), the doses will be significantly different. In such a situation, using the VMAT technique, one will provide a dose larger by approximately 0.41 Gy on the target and up to 9.59 Gy on the brainstem throughout the entire treatment cycle as compared with the conformal technique. The conformal technique will provide a dose higher by approximately 0.19 Gy in both eyes and by about 5.13 Gy in the brain.

Chest area

Comparing the two treatment techniques, a higher dose of 0.12 Gy in the target area and of 0.22 Gy in the right lung for the VMAT technique can be noted. However, if we apply the criterion of protection of the heart and the vertebral bone, the doses at these points are lower by 0.12 Gy (heart) and 0.03 Gy (vertebral bone) for the VMAT technique.

In a 23 fractions case, using the VMAT technique throughout the whole treatment cycle, the target would obtain a dose higher by approximately 2.67 Gy and the right lung by as much as 4.97 Gy in comparison with the conformal technique. The conformal technique will provide a larger dose of approximately 2.76 Gy in the heart and of approximately 0.57 Gy in the bone with a spinal canal.

Pelvic area

Comparison of the two treatment techniques shows that a higher dose of 0.02 Gy in the target area and

of 0.07 Gy in the rectum for the VMAT technique can be observed. However, if we adopt the criterion of protection of the femoral heads, the doses at these points are lower by 0.10 Gy for the VMAT technique.

For the 38 fractions, the doses will be significantly different. In such a case, using the VMAT technique throughout the whole treatment cycle, the target would obtain a dose higher by approximately 0.87 Gy and the rectum by as much as 2.58 Gy in comparison with the conformal technique. The conformal technique will provide a larger dose of approximately 3.59 Gy in the femoral heads.

Conclusions

All the treatment plans were verified using TLDs, and it can be stated that the doses in the target and in the critical organs are consistent with the doses given in the TPS.

As regards the comparison of the two treatment techniques, a more homogeneous dose distribution and its increase in the target for all the tumours under investigation can be observed in the VMAT technique rather than in the conformal technique. On the whole, it is beneficial given the full irradiation of the tumour.

VMAT allows reducing dose in most OARs without compromising target coverage [9].

According to various authors, VMAT seems to be the optimal treatment planning technique in the dosimetric comparison with different treatment methods in lung or breast cancer [10, 11]. It allows maximal lung and heart sparing when compared to the conformal technique. In addition, it allows dose escalation when needed, with minimal increased dose to OARs. The main concern when using VMAT is the spreading of low-radiation dose to the normal tissue and hence an increased integral dose. This raises concerns of possible increased risk of secondary cancer. The calculated doses to the OARs in head and neck and pelvic area were considerably lower with VMAT than with the conformal technique. Therefore, the estimated risk for secondary cancer should be considerably lower with VMAT for this area, which is consistent with other publications [12]. Although there is evidence to show that VMAT has a definite place in the treatment of many tumours, it cannot be considered the universal solution for all clinical scenarios because each case must be evaluated on an individual basis to select the most appropriate radiation technique that will give optimal results.

ORCID

M. Paluch-Ferszt  <http://orcid.org/0000-0003-1839-0409>

References

1. Li, J. -S., Pawlicki, T., Deng, J., Jiang, S. -B., Mok, E., & Ma, C. -M. (2000). Validation of a Monte Carlo dose

- calculation tool for radiotherapy treatment planning. *Phys. Med. Biol.*, 45(10), 2969–2985. DOI: S0031-9155(00)12262-6.
2. Oelkfe, U., & Scholz, C. (2006). Dose calculation algorithms. In W. Schlegel, T. Bortfeld, & A. -L. Grosu (Eds.), *New technologies in radiation oncology* (pp.187–196). Berlin-Heidelberg: Springer.
3. Wu, V. -W., Tse, T. -K., Ho, C. -L., & Yeung, E. -C. (2013). A comparison between anisotropic analytical and multigrad superposition dose calculation algorithms in radiotherapy treatment planning. *Med. Phys.*, 38(2), 209–214. DOI: 10.1016/j.meddos.2013.02.001.
4. International Atomic Energy Agency. (2004). *Commissioning and quality assurance of computerized planning systems for radiation treatment of cancer*. Vienna: IAEA. (TRS No 430).
5. Rogers, D. -W. -O., & Bielajew, A. -F. (1990). Monte Carlo techniques of electron and photon transport for radiation dosimetry. In K. -R. Kase, B. -E. Bjarngard, & F. -H. Attix (Eds.), *The dosimetry of ionizing radiation* (pp. 427–540). Canada: Academic Press.
6. Ahnesjö, A. (1989). Collapsed cone convolution of radiant energy for photon dose calculation in heterogeneous media. *Med. Phys.*, 16(4), 577–592. DOI: 10.1118/1.596360.
7. Krieger, T., & Sauer, O. -A. (2005). Monte Carlo versus pencil-beam-/collapsed-cone-dose calculation in a heterogeneous multi-layer phantom. *Phys. Med. Biol.*, 50(5), 859–868. DOI: 10.1088/0031-9155/50/5/010.
8. Mijnheer, B., Olszewska, A., Fiorino, C., & Welleweerd, H. (2004). *Quality assurance of treatment planning systems, practical examples for non-IMRT photon beams*. Brussels: European Society of Therapeutic Radiation Oncology.
9. Haertl, P. M., Pohl, F., Weidner, K., Groeger, Ch., Koelbl, O., & Dobler, B. (2013). Treatment of left sided breast cancer for a patient with funnel chest: Volumetric-modulated arc therapy vs. 3D-CRT and intensity-modulated radiotherapy. *Med. Dosim.*, 38(1), 1–4. DOI: 10.1016/j.meddos.2012.04.003.
10. Xu, Y., Deng, W., Yang, S., Li, P., Kong, Y., Tian, Y., Liao, Z., & Chen, M. (2017). Dosimetric comparison of the helical tomotherapy, volumetric modulated arc therapy and fixed-field intensity-modulated radiotherapy for stage IIB-IIIB nonsmall cell lung cancer. *Sci. Rep.*, 7(1), 14863. DOI: 10.1038/s41598-017-14629-w.
11. Abo-Madyan, Y., Aziz, M. H., Aly, M. M. O. M., Schneider, F., Sperk, E., Clausen, S., Giordano, F. A., Herskind, C., Steil, V., Wenz, F., & Glatting, G. (2014). Second cancer risk after 3D-CRT, IMRT and VMAT for breast cancer. *Radiother. Oncol.*, 110(3), 471–476. DOI: 10.1016/j.radonc.2013.12.002.
12. Rehman, J. U., Isa, M., Ahmad, N., Nasar, G., Asghar, H. M., Gilani, Z. A., Chow, J. C., Afzal, M., & Ibbott, G. S. (2018). Dosimetric, radiobiological and secondary cancer risk evaluation in head-and-neck three-dimensional conformal radiation therapy, intensity-modulated radiation therapy, and volumetric modulated arc therapy: A phantom study. *J. Med. Phys.*, 43(2), 129–135. DOI: 10.4103/jmp.JMP_106_17.